NeuroImage 56 (2011) 709–715

Contents lists available at ScienceDirect

NeuroImage

journal homepage: www.elsevier.com/locate/ynimg

Decoding different roles for vmPFC and dlPFC in multi-attribute decision making

Thorsten Kahnt [a,b], Jakob Heinzle [a], Soyoung Q. Park [b,c], John-Dylan Haynes [a,b,d,*]

[a] Bernstein Center for Computational Neuroscience, Charité-Universitätsmedizin Berlin, Germany
[b] Berlin School of Mind and Brain, Humboldt Universität zu Berlin, Germany
[c] Department of Education and Psychology, Freie Universität, Berlin, Germany
[d] Max Planck Institute for Human Cognitive and Brain Sciences, Leipzig, Germany

ARTICLE INFO

Article history:
Received 18 March 2010
Revised 30 April 2010
Accepted 20 May 2010
Available online 25 May 2010

Keywords:
Multi-attribute decision making
Expected value
Functional magnetic resonance imaging (fMRI)
Multivariate decoding
Ventromedial prefrontal cortex (vmPFC)
Dorsolateral prefrontal cortex (dlPFC)

ABSTRACT

In everyday life, successful decision making requires precise representations of expected values. However, for most behavioral options more than one attribute can be relevant in order to predict the expected reward. Thus, to make good or even optimal choices the reward predictions of multiple attributes need to be integrated into a combined expected value. Importantly, the individual attributes of such multi-attribute objects can agree or disagree in their reward prediction. Here we address where the brain encodes the combined reward prediction (averaged across attributes) and where it encodes the variability of the value predictions of the individual attributes. We acquired fMRI data while subjects performed a task in which they had to integrate reward predictions from multiple attributes into a combined value. Using time-resolved pattern recognition techniques (support vector regression) we find that (1) the combined value is encoded in distributed fMRI patterns in the ventromedial prefrontal cortex (vmPFC) and that (2) the variability of value predictions of the individual attributes is encoded in the dorsolateral prefrontal cortex (dlPFC). The combined value could be used to guide choices, whereas the variability of the value predictions of individual attributes indicates an ambiguity that results in an increased difficulty of the value-integration. These results demonstrate that the different features defining multi-attribute objects are encoded in non-overlapping brain regions and therefore suggest different roles for vmPFC and dlPFC in multi-attribute decision making.

Introduction

Successful decision making requires precise anticipatory representations of the reward values that can be obtained from choosing specific behavioral options. However, in everyday life most decision alternatives consist of multiple reward-related attributes. For instance, different attributes of a fruit–size, shape, color and surface texture–signal parts of its nutritional value. To make an optimal choice i.e. to pick the fruit with the highest expected value, the reward predictions of all attributes need to be integrated into a combined value. To describe such decision processes, Multi-Attribute Utility Theory (MAUT) was developed by behavioral decision researchers in the 1970s (Slovic et al., 1977; von Winterfeldt and Fischer, 1975).

Neuroscience has mainly focused on decisions regarding single-attribute options (Daw et al., 2006; Glascher et al., 2009; Hampton et al., 2006; Kim et al., 2006; O'Doherty et al., 2003b). Studies on multiple attributes have typically directly investigated the trade-off between two attributes such as taste vs. health (Hare et al., 2009), amount of money vs. delay (Kable and Glimcher, 2007) and pleasure of acquisition vs. price (Knutson et al., 2007). Furthermore, studies on decisions between real-life objects (comprising multiple attributes) typically did not address their multiple-attribute character explicitly (Chib et al., 2009; FitzGerald et al., 2009; Hare et al., 2009; Knutson et al., 2007; Plassmann et al., 2007). One study aimed to identify brain regions involved in experimentally controlled multi-attribute decisions (Zysset et al., 2006). In this study, however, only the attribute-wise similarity between alternatives i.e. the difficulty of the decision was examined. Taken together, although single- and two-attribute decisions have been studied, no study has moved beyond two attributes and comprehensively investigated how such multi-attribute objects are represented in the brain.

Each attribute of a multi-attribute object can have its own predictive information for reward. Importantly, different attributes of the same object can signal *different or even conflicting* reward values. For instance, for one object all attributes could signal an intermediate value, whereas for another object different attributes could signal high and low values. Thus, although both objects have the same combined value (i.e. intermediate) the multi-attribute objects would differ considerably in the *variability* of the rewards predicted by their individual attributes (i.e. low vs. high). Hence, unlike single-attribute objects, different multi-attribute objects can differ not only in their expected value but also in the variability of the rewards predicted by their attributes. In order to understand how decisions are made on the basis of multi-attribute objects we investigated how the

* Corresponding author. Charité-Universitätsmedizin Berlin, Bernstein Center for Computational Neuroscience, Haus 6, Philippstrasse 13, 10115 Berlin.
E-mail address: haynes@bccn-berlin.de (J.-D. Haynes).

1053-8119/$ – see front matter © 2010 Elsevier Inc. All rights reserved.
doi:10.1016/j.neuroimage.2010.05.058

combined value and the variability of the rewards predicted by the individual attributes are represented in the human brain.

Recently we have shown that expected values can be decoded from distributed fMRI patterns in the ventromedial prefrontal cortex (vmPFC) (Kahnt et al., 2010). This distributed coding is consistent with reports from single-unit recordings showing that different neural populations in value sensitive cortex increase and decrease their firing rate with increasing reward value, respectively (Kennerley et al., 2009; Kobayashi et al., 2010; Morrison and Salzman, 2009; Padoa-Schioppa and Assad, 2006; Schoenbaum et al., 2007). Previous experimental and theoretical work on the human visual system has revealed that applying multivariate pattern analysis (MVPA) techniques to fMRI data is specifically suited to extract information encoded in distributed neural populations (Haynes and Rees, 2005, 2006; Kamitani and Tong, 2005; Norman et al., 2006). Similarly, information about cognitive and decision processes has been shown to be encoded in distributed fMRI patterns in the prefrontal cortex (PFC) (Hampton and O'Doherty, 2007; Haynes et al., 2007; Soon et al., 2008). Thus, it might be expected that distributed fMRI patterns contain more information about the combined value of multi-attribute objects and the variability of rewards predicted by individual attributes than the average fMRI signal. Hence, here we used MVPA techniques (Haynes and Rees, 2006; Norman et al., 2006) to decode information about these two variables.

Materials and methods

Participants

Sixteen right-handed subjects (8 female, mean age = 26.4 ± 1.06 years SEM) participated in the experiment. Subjects had normal or corrected-to-normal vision and gave written informed consent to participate. The study was approved by the local ethics review board of the Charité-Universitätsmedizin Berlin.

Classical conditioning session

In all experiments we used objects that could vary in three visual attributes *shape*, *color* and *coherence of moving dots* with three levels per attribute. In the days prior to scanning (mean 3.19 ± 0.31 SEM) participants performed a *classical conditioning session*, where they learned the association between *single-attribute objects* and different reward values (magnitudes of monetary outcomes). For this behavioral session the objects had only a single feature that varied across three levels, thus resulting in 9 stimuli (3 × shape + 3 × color + 3 × coherence). The three different shapes (diamond, octagon and dodecagon) were presented in white color on black background, the three colors (green, turquoise and blue) were presented in squares on black background and the three coherence levels of moving dots (5%, 35% and 95% coherence) were also presented in white squares on black background (Fig. 1B). The three levels of each attribute were associated with increasing magnitudes of monetary outcomes (0.10 €, 0.20 € and 0.30 €). An example pairing is shown in Fig. 1B; the actual pairings were counter-balanced across subjects and gender. During conditioning, in each trial one single-attribute object (e.g. a green square indicating 0.10 €) was randomly selected and presented for 2000 ms followed by the presentation of its monetary value (1000 ms). Subjects were told that they will receive the money after the experiment. Each stimulus was presented 10 times, resulting in 90 conditioning trials.

Scanning session

In each trial of the fMRI experiment (Fig. 1A), one level of every single-attribute was combined into a *multi-attribute object* (e.g. shape: octagon indicating 0.20 €, color: blue indicating 0.30 € and coherence: 5% indicating 0.10 €) and presented for 2000 ms. After a variable delay (4000–8000 ms) subjects were asked to rate the combined value of that object on a continuous, circular rating scale (without labeling) using an MRI compatible trackball. Once the rating was made the cursor was blocked and the rating scale stayed presented for a total of 2500 ms (maximum rating time). In the scanning session the objects consisted of *combinations* of all three attribute levels, thus resulting in 27 different multi-attribute objects (3 × 3 × 3 = 27). Each was presented two times in each of the 4 scanning runs. Subjects were informed that they would receive 50% of the combined value (sum of single-attribute values) of each multi-attribute object they evaluated during the experiment. Before scanning, subjects repeated the conditioning procedure described above and practiced on the circular rating scale. Furthermore, they went through one run (54 trials) of the experiment as a practice.

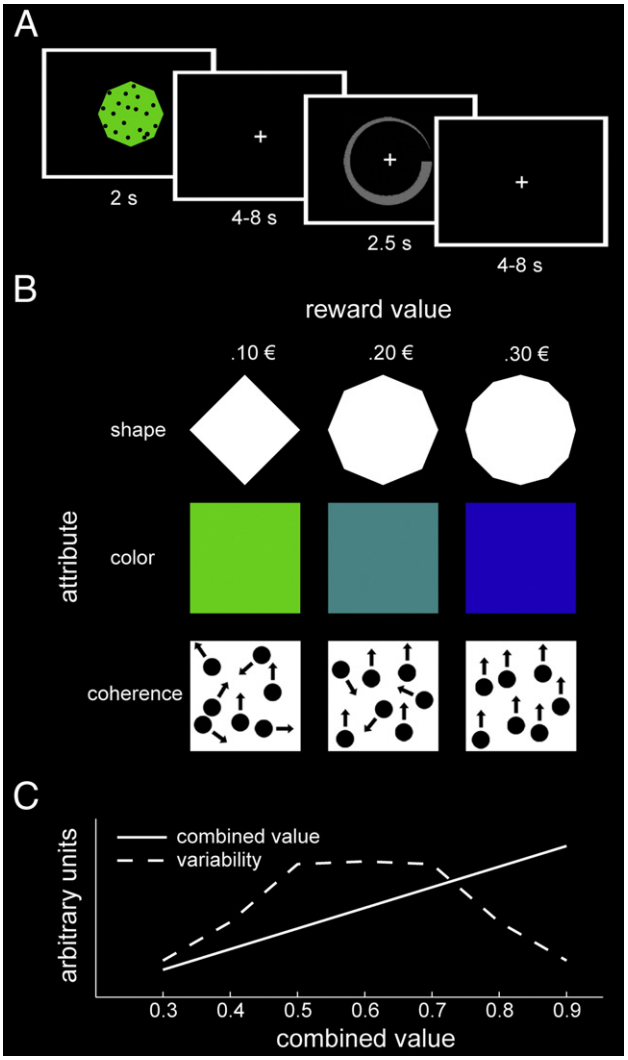

Fig. 1. Experimental design. (A) Example trial of the task used in the scanner. In each trial one multi-attribute object was presented for 2 s. After a variable delay of 4–8 s subjects had to rate the combined value of the object (maximum rating time 2.5 s). Trials were separated by a variable interval of 3.5–7.5 s. To avoid motor preparation and confounds related to the motor component of the rating, a circular rating scale with randomized orientation was used. (B) Example of associations between single attributes and rewards. Different rows indicate the attributes shape, color and coherence (of moving dots) and columns indicate the reward value that was associated with the visual cues in the cells during the classical conditioning procedure. Associations were counter-balanced across subjects and gender. (C) Average relationship between the combined value and the variability of multi-attribute objects. Combined value (solid line) and variability (dashed line) are plotted as a function of combined value.

Combined value and variability of multi-attribute objects

For each of the 27 multi-attribute objects the *mean value* and the *variability* of the rewards predicted by the individual attributes was computed and constituted the variables of interest in our study. For each multi-attribute object *j* the combined value $\overline{x}$ was defined as the mean of the reward predictions *x* associated with its attributes *i*….*n*:

$$\bar{x}_j = \sum_i x_i \cdot \frac{1}{n}$$

It is important to note that defining the combined value as mean or the sum of the single-attributes does not affect the results because both variables are perfectly correlated. However, because evidence suggests that animals tend to add rather then average reward predictions from multiple cues (Lattal and Nakajima, 1998; Rescorla, 1970), subjects were told that the reward predictions were additive. For each multi-attribute object *j* the variability σ^2 was defined as the mean squared difference between the reward predictions *x* of the attributes *i*….*n* and the combined value $\overline{x}$:

$$\sigma_j^2 = \sum_i \left(\bar{x} - x_i \right)^2 \cdot \frac{1}{n}$$

Importantly, the combined value and the variability are orthogonal and thus both variables can be decoded independently of each other (see Fig. 1C).

fMRI acquisition and pre-processing

Functional imaging was conducted on a 3-Tesla Siemens Trio (Erlangen, Germany) scanner equipped with a 12-channel head coil. In each run, 420 T2*-weighted gradient-echo echo-planar images (EPI) containing 33 slices (3 mm thick) separated by a gap of 0.75 mm were acquired. Imaging parameters were as follows: repetition time (TR) 2000 ms, echo time (TE) 30 ms, flip angle 90°, matrix size 64×64 and a field of view (FOV) of 192 mm, resulting in a voxel size of 3 by 3 by 3.75 mm. A T1 weighted structural data set was collected for the purpose of anatomical localization. The parameters were as follows: TR 1900 ms, TE 2.52 ms, matrix size 256×256, FOV 256 mm, 192 slices (1 mm thick), flip angle 9°.

Preprocessing, first-level general linear model (GLM) and second-level group statistics were performed using SPM2 (Wellcome Department of Imaging Neuroscience, Institute of Neurology, London, UK). The first three volumes of each run were discarded to allow for magnetic saturation effects. For preprocessing, images were slice time corrected and realigned. Importantly, no spatial normalization or smoothing was applied at this point of the analysis.

Time-resolved searchlight decoding of combined value and variability

To identify where in the brain information about the *combined value* and the *variability of reward-prediction* of individual attributes is encoded, we used a time-resolved multivariate decoding technique which has been described previously (Bode and Haynes, 2009; Haynes et al., 2007; Kriegeskorte et al., 2006; Soon et al., 2008). First, preprocessed data was analyzed using a general linear model (GLM). For each run a finite impulse response (FIR) model was fitted to the data (Ollinger et al., 2001). Trials were sorted according to their combined value into seven groups. These seven groups of trials as well as the rating scale were each modeled using 10 FIR regressors covering the 20 s after the onset of the multi-attribute object. These regressors were then simultaneously regressed against the BOLD signal in each voxel. The resulting parameter estimates in each voxel represent the response amplitude for each of the seven value levels at ten different time points after the onset of the multi-attribute object.

The spatial patterns of estimated response amplitudes from each time point were then used to search for brain regions that carry spatially distributed information about the combined value of multi-attribute objects. For this, we used a "searchlight" approach (Haynes et al., 2007; Kriegeskorte et al., 2006) which examines the information in local fMRI patterns surrounding each voxel v_i (see Fig. 2 for an illustration of the procedure). This approach allows extraction of information from locally distributed fMRI patterns without potentially biasing prior voxel selection. For a given voxel v_i we first defined a small spherical cluster of radius = 4 voxels centered on v_i. For each voxel in this local cluster we extracted the unsmoothed parameter estimates separately for all subjective value levels, and separately for all 10 time points *t*. This yielded seven N-dimensional pattern vectors for each run and each time point *t*, representing the spatially distributed response patterns of different value levels in the local cluster. We then used 3 of the 4 runs to train a linear support vector regression (SVR) to predict the value of the multi-attribute objects from these local response patterns. The value related information encoded within a local cluster was then assessed by examining how well the combined value levels in the remaining independent "test" data set were predicted by the SVR model. Specifically, *prediction accuracy* was defined as the Fisher's Z-transformed correlation coefficient between the predicted value levels and the actual value levels of the test data set. In total, the training and test procedure was repeated four times, each with a different run assigned as test data set yielding an average prediction accuracy in the local environment of the central voxel v_i (4-fold cross-validation). This procedure was repeated for all time points *t* and all spatial positions, i.e. voxels v_j. For each subject, this resulted in 10 maps of prediction accuracy, one for each time point after the onset of the multi-attribute object. The SVR was performed using the LIBSVM implementation (http://www.csie.ntu.edu.tw/~cjlin/libsvm) with a linear kernel and a constant regularization parameter of $c = 1$. To identify where in the brain information about the variability of value predictions is encoded, we used the same time-resolved searchlight approach described above. This time, however, trials were sorted according to their variability into four groups and the level of variability was decoded at different spatial positions and time points.

For the second-level analyses the accuracy maps from the decoding were normalized based on parameters obtained from normalizing the EPI images to the MNI template and smoothed with a 6 mm FWHM Gaussian kernel (Haynes et al., 2007). The normalized and smoothed accuracy maps for combined value and variability were then entered into separate one-way ANOVAs with 10 levels (one for each time point), respectively. To identify regions that contained significant information about the combined value and variability of reward predictions we performed voxel-wise *t*-tests on time points 2–4 after stimulus onset. This time window was chosen because during time points 2–4 BOLD responses to the multi-attribute objects are independent of BOLD responses to the subsequent rating period. We report significant voxels surviving a threshold of $p < 0.0001$, uncorrected with a cluster extend threshold of $k = 15$ continuous voxels that survive correction for multiple comparisons at the cluster level ($p < 0.05$) as implemented in SPM2.

Results

In this section we first report the behavioral results and show how the combined value and the variability of the multi-attribute objects are reflected in subjects' behavior. We then proceed to show how the combined value and variability are encoded in the brain. We find that non-overlapping brain regions, the ventromedial PFC (vmPFC) and the dorsolateral PFC (dlPFC), respectively, contain information about these variables that characterize multi-attribute objects.

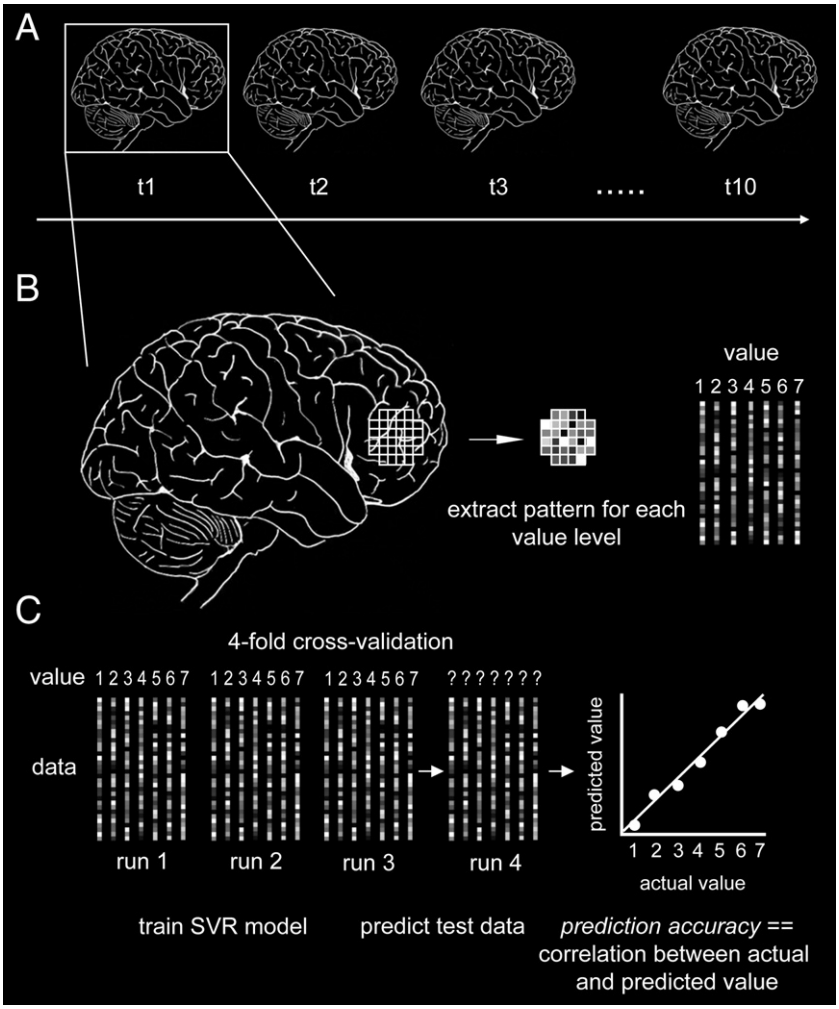

Fig. 2. Time-resolved searchlight decoding. (A) The decoding procedure was performed for each time point *t* separately. (B) For a given time point *t* and voxel *i*, a spherical cluster (searchlight with radius $k=4$ voxels) surrounding voxel *i* was defined and parameter estimates (from a finite impulse response model) of each combined value level and each run were extracted, resulting in seven N-dimensional pattern vectors for each scanning run. (C) Three of the 4 runs were assigned to a training data set that was used to train a linear support vector regression (SVR). The SVR model was then used to predict the combined value of the remaining independent test data set. The *prediction accuracy* of the SVR model was then computed as the Fisher's Z-transformed correlation coefficient between the actual value of the test data and the value predicted by the SVR model. This procedure was repeated 4 times, each time assigning a different run as the independent test data set, resulting in average prediction accuracy for the local cluster surrounding voxel *i* (4-fold cross-validation). Then the whole procedure was repeated with the next voxel $i+1$ as searchlight center. The same procedure was also used to decode information about the variability of the reward predictions of the multi-attribute objects.

Behavioral results

Value ratings of the multi-attribute objects increased linearly with increasing combined value (Fig. 3A). In Fig. 3C the subjective ratings are plotted as a function of the single-attribute value for all three attributes. Ratings increased linearly with all three single-attributes. To assess this effect on a single-subject level, we regressed the three single-attribute values simultaneously against the trial-wise ratings. This multiple regression model was significant in every subject ($p<0.001$, average $R^2=0.75\pm0.04$, SEM) which suggests that subjects integrated the different reward predictions linearly into a combined value.

Fig. 3B depicts the relationship between RT and the variability of the reward predictions. We regressed the variability against the trial-wise RT; across subjects the slope of this regression was significantly positive (average slope $=61.85$, $t=2.67$, $p<0.05$). Thus, subjects needed more time to rate the combined value in trials where the variability of the reward predictions was high. This might indicate that rating multi-attribute objects with contradicting reward predictions is more difficult than rating objects with coherent reward predictions.

fMRI decoding results

Using the time-resolved searchlight approach and SVR we examined where in the brain distributed fMRI patterns contained information about the *combined value* of the multi-attribute objects. Because the combined value of the objects is correlated with the visual properties of the attributes, we masked out brain regions that carry information about the visual properties of the attributes. The exclusive mask consisted of all voxels in which significant ($p<0.005$) information about any of the three single attributes was decoded (using a linear SVR, see Fig. S1). During scans 2–4 after stimulus onset we found significant ($p<0.0001$, uncorrected with a cluster extend threshold of $k=15$, surviving a corrected threshold of $p<0.05$ at the cluster level) information about value in the vmPFC (BA 10/11, [−6, 51, −6], $t=4.26$, Fig. 4A). For illustration purposes, the graph on the right in Fig. 4A depicts the temporal profile of value encoding in the vmPFC. In this region value information was present during the presentation of the multi-attribute object but not during the subsequent rating period.

Because the visual attributes are correlated with their value (within each subject), an alternative explanation for our result of

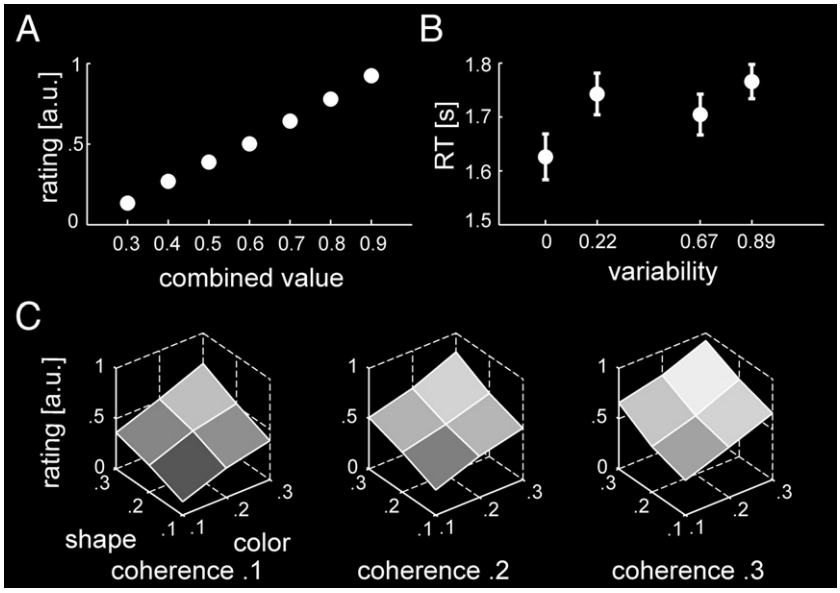

Fig. 3. Behavioral results. (A) Ratings plotted as a function of combined value (sum of single-attribute reward predictions). Error bars for SEM are smaller than the symbols. (B) Reaction time (RT) of the ratings plotted as a function of the variability of reward predictions. Error bars depict SEM. (C) Subjective ratings as a function of the value of the single attributes shape (*x*-axis), color (*y*-axis) and coherence (different diagrams from left to right).

value signals in the vmPFC is that not the combined value of the objects but rather the visual attributes are encoded. To rule out this explanation, we trained a classifier to dissociate different multi-attribute objects all having the same intermediate value. This analysis was performed for all possible pair-wise combinations of multi-attribute objects with the same intermediate combined value. In the vmPFC, classifier performance was at chance ($t=-0.69$, $p=0.50$), suggesting that the combined values are held in working memory in the vmPFC rather than the visual attributes of the stimulus.

We compared this result to a more conventional voxel-wise analysis using a GLM with a parametric regressor for the combined values of the multi-attribute objects. In this analysis no clusters revealed significant correlations with the combined value at our threshold ($p<0.0001$, $k=15$). Furthermore, we estimated the amount of value-related information present in the average signal of each searchlight by decoding the combined value from the average signal (mean signal across all voxels in a given searchlight). In the vmPFC, decoding performance using this average signal was at chance ($t=0.57$, $p=0.58$). This shows that in the context of the current experiment, there is no significant value-related information in the average signal of the vmPFC, whereas the combined value is robustly represented in the multivariate activity patterns in this region.

In the next analysis we searched for brain regions that contained information about the *variability* of multi-attribute objects. During scans 2–4 after stimulus onset we found significant ($p<0.0001$, uncorrected with a cluster extend threshold of $k=15$, surviving a corrected threshold of $p<0.05$ at the cluster level) information about the variability of the reward predictions in the dlPFC (BA 45/46, left dlPFC, [−33, 24, 24], $t=5.30$, Fig. 4B), the dorsomedial parietal cortex (dmPC BA 2/5, [3, −36, 69], $t=4.73$, Fig. 4C) and the cerebellum (left cerebellum, [−39, −57, −36], $t=4.46$; right cerebellum, [36, −63, −27], $t=4.38$). For illustration purposes, the right columns of Fig. 4B+C depict the temporal profile of encoding in the left dlPFC and the dmPC, respectively. It can be seen that information about the variability in the dlPFC and dmPC can be decoded during the presentation of the multi-attribute object but also during the subsequent rating period.

As reported above, subjects responded with longer RTs with increasing variability of the value predictions. Thus it is unclear whether dlPFC and dmPC encode variability per se or rather sustained attention while making a more difficult decision. To test this idea we controlled for the RT component in the data by regressing out RT from the voxel-wise responses prior to decoding. After controlling for RT, information about the variability in the dlPFC and dmPFC, but not the cerebellum was still significant at the same threshold of $p<0.0001$ (dlPFC BA 45/46, [−33, 24, 24], $t=4.25$ and dmPC BA 2/5, [3, −39, 66], $t=3.88$). This result shows that variability is encoded independent of RT in the dlPFC and dmPC, suggesting a role for these regions in coding the variability of value predictions independent of the behavioral demands.

Again, these results were also compared to a more conventional univariate analysis using a GLM with a parametric regressor for the variability of the value predictions. In this whole-brain analysis no cluster revealed significant correlations with the variability at our threshold ($p<0.0001$, $k=15$). Furthermore, decoding the variability of the value predictions from the average searchlight signals in the dlPFC and the dmPC was at chance ($t=-0.22$, $p=0.83$ and $t=-0.57$, $p=0.58$, for dlPFC and dmPC, respectively). This suggests that at least in the context of the current task, the average signal in the dlPFC and dmPC contains no information about the variability of the value predictions, highlighting the importance of using multivariate analysis methods.

Discussion

In the current experiment we demonstrate that two variables characterizing multi-attribute objects are encoded in different brain regions, the vmPFC and the dlPFC. Whereas the *combined value* is represented in the vmPFC, the *variability* of the reward predictions of the individual attributes is encoded in the dlPFC. A previous study identified a network of brain regions including the medial PFC and the dlPFC that was involved in multi-attribute decision making (Zysset et al., 2006). Based on the activity time-courses in these regions this study concluded that medial PFC and dlPFC are related to the "control level" of decision making. However, using analysis methods that are sensitive to information rather than activation, our results suggest orthogonal rather than common roles for both regions.

Information about the *combined value* of multi-attribute objects was encoded in distributed fMRI patterns in the vmPFC. Using single- or two-attribute objects, previous neuroimaging studies in humans also identified this region in which activity correlates with estimates

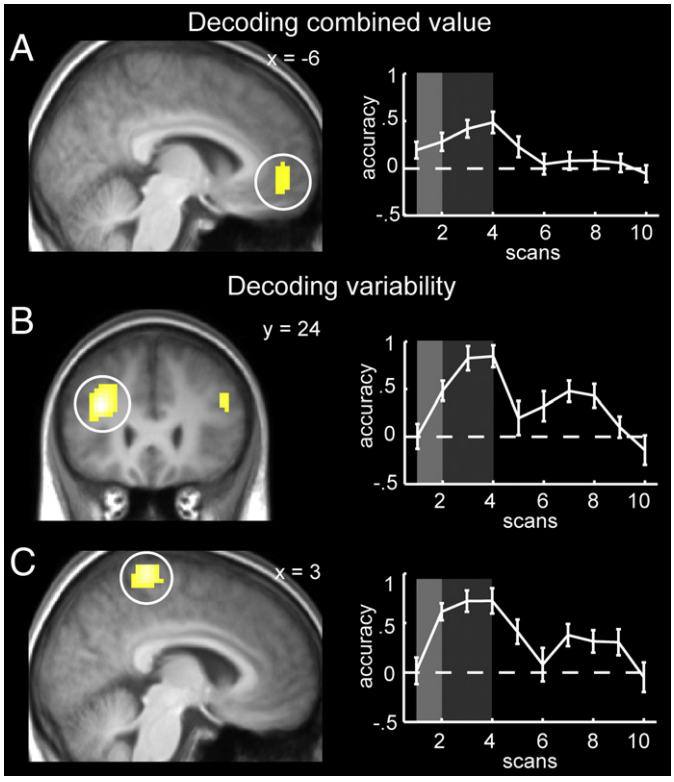

Fig. 4. Decoding combined value and variability of multi-attribute objects. Group statistics on prediction accuracy (Fisher's *Z*-transformed correlation coefficients) averaged over scans 2–4. (A) Significant information about combined value was decoded from the vmPFC (MNI coordinates [*x*, *y*, *z*], [−6, 51, −6], $t=4.26$). (B) Significant information about the variability of the value predictions was decoded in the left dlPFC ([−33, 24, 24], $t=5.30$) and (C) the dorsomedial parietal cortex (dmPC, [3, −36, 69], $t=4.73$). The cluster in the right dlPFC in (B) ([45, 27, 27], $t=4.17$) does not survive correction for multiple comparisons at the cluster level ($p=0.12$). For illustration purposes, *t*-maps are thresholded at $p<0.0001$ uncorrected with a cluster extend threshold of $k=15$ and overlaid on a normalized structural image averaged across subjects. The graphs on the right depict prediction accuracy (Fisher's *Z*-transformed correlation coefficients) from the individual peak voxels within the cluster on the left (white circle) is plotted as a function of time (scans) (for illustration purposes only). Bright shaded areas depict the presentation of the multi-attribute object. BOLD responses to the objects during scans 2–4 (dark shaded areas) were unaffected by the rating period.

of value (Behrens et al., 2007; Breiter et al., 2001; Cohen et al., 2008; Daw et al., 2006; Gottfried et al., 2003; Kable and Glimcher, 2007; Kahnt et al., 2009, 2010; Kim et al., 2006; Yacubian et al., 2006). Furthermore, activity in vmPFC has also been shown to increase with the value of everyday objects which typically comprise multiple value-related attributes (Chib et al., 2009; Hare et al., 2009; Knutson et al., 2007; Plassmann et al., 2007). For example, Hare et al. (2009) demonstrated that the value of snacks which is determined not only by taste but also by health judgments is correlated with activity in the vmPFC. These studies have also argued that vmPFC encodes the overall value of an item, integrating over multiple and often conflicting attributes. Here we moved beyond two attributes and used pattern recognition techniques to investigate the representation of the combined value. On the other hand, however, a consistent finding across electrophysiological studies in animals investigating the representation of value is that different populations of neurons encode the positive and negative value of cues, respectively. Typically, about 50% of value sensitive neurons increase their firing rate with increasing value, whereas the other half decrease their firing rate with increasing value (Kennerley et al., 2009; Kobayashi et al., 2010; Morrison and Salzman, 2009; Padoa-Schioppa and Assad, 2006; Schoenbaum et al., 2007). Averaging the signal from neural populations that are equally prevalent but exhibit opposing encoding schemes within individual fMRI voxels could average out the signal of interest leaving only a slight response bias, as argued previously (Kennerley et al., 2009). Indeed, information about expected reward can be decoded from patterns of such response biases in the vmPFC using multivariate pattern classification (Kahnt et al., 2010). Here, we extend this finding by showing that distributed fMRI patterns in the vmPFC can be used to make linear predictions about the combined value of multi-attribute objects.

Values are the crucial element in reinforcement learning algorithms (Sutton and Barto, 1998) and play an important role for decision making and adaptive behavior (Cohen, 2008; Montague et al., 2004). To make optimal choices, it is essential to represent the expected value of objects or actions. The combined reward prediction of multi-attribute objects could be represented in the vmPFC as subjective or economic value where it can be used to guide choices (Kable and Glimcher, 2007; Montague and Berns, 2002; Padoa-Schioppa and Assad, 2006). Furthermore, expected values are compared with the value of the actual outcome, leading to errors of reward prediction that are necessary for learning and adaptive behavior. These prediction errors are coded by dopaminergic neurons in the ventral tegmental area (Bayer and Glimcher, 2005; Schultz et al., 1997; Takahashi et al., 2009) and are thought to update the expected value of stimuli or actions in the striatum (Kahnt et al., 2009; McClure et al., 2003; O'Doherty et al., 2003a; Pessiglione et al., 2006).

The second feature characterizing multi-attribute objects is the *variability* of the rewards predicted by the individual attributes. If all attributes of an object signal similar values the variability of the reward predictions is low, if, however, attributes make contradicting value predictions the variability is high. Thus, the higher the variability the more ambiguous is the combined value prediction of the multi-attribute object. In our study, the variability was encoded in the dlPFC. This is consistent with a recent report showing activity in dlPFC to be correlated with ambiguous cues (Bach et al., 2009). On a behavioral level, high variability was associated with longer RT which implies a relationship between variability and the difficulty of integrating multiple reward predictions. The encoding of variability in the dlPFC suggests that this region is sensitive to the difficulty of the integration process. Thus dlPFC could be directly involved in the integration of multiple reward predictions into a combined value. Previous work in animals and humans has revealed integration processes in the dlPFC that support perceptual choices (Gold and Shadlen, 2007; Heekeren et al., 2008; Romo and Salinas, 2003). Specifically, neurons in the primate dlPFC sustain memory traces of sensory information (Goldman-Rakic, 1987; Romo et al., 1999) and fMRI signals in the human dlPFC reflect the integrated evidence from higher sensory cortices (Heekeren et al., 2004). Together with these results, our data point towards a more general role of dlPFC in integration processes during decision making which is not restricted to perceptual choices but generalizes to reward-based decisions.

We cannot completely resolve an ambiguity in the interpretation of our results. It remains unknown whether encoding of value in vmPFC and variability in dlPFC would be the same if the rating task had not been added after the presentation of the multi-attribute object. It could be the case that vmPFC encodes the combined reward prediction only because it is used to construct the rating and dlPFC could encode variability only because it is correlated with the difficulty of coming up with this rating. Alternatively, these regions could encode the combined value and variability of the reward predictions irrespective whether or not the subjects had to make any response at all. However, because decoding was robust when controlling for RT, at least variability in dlPFC seems to be independent of the task demands as reflected in the RTs.

In multi-attribute decision making each attribute of an object can signal its own reward prediction. Thus, such objects could be described as *distribution of reward predictions*. The combined value and the variability investigated in the current study correspond to the

1st and 2nd moment (*mean* and *variance*) of such distributions, respectively. These two moments are required to effectively characterize the reward predictions of multi-attribute objects comprehensively. To conclude, here we have shown that these two moments, the combined value and the variability are encoded in two different brain regions, the vmPFC and the dlPFC, respectively. Our results suggest that dlPFC signals ambiguity and is likely to be involved in the integration of value predictions into a combined value. VMPFC on the other hand represents the combined value that could directly guide choices. By showing how multi-attribute objects are comprehensively represented in the human brain, our study provides an important step in understanding how decisions are made on the basis of multi-attribute objects. Further studies need to show how these findings extend to qualitatively different incentives of different attributes and how actual choices are made based on such multi-attribute representations.

Acknowledgments

This work was funded by the Bernstein Computational Neuroscience Program of the German Federal Ministry of Education and Research (BMBF Grant 01GQ0411), the Excellence Initiative of the German Federal Ministry of Education and Research (DFG Grant GSC86/1-2009) and the Max Planck Society.

Appendix A. Supplementary data

Supplementary data associated with this article can be found, in the online version, at doi:10.1016/j.neuroimage.2010.05.058.

References

Bach, D.R., Seymour, B., Dolan, R.J., 2009. Neural activity associated with the passive prediction of ambiguity and risk for aversive events. J. Neurosci. 29, 1648–1656.
Bayer, H.M., Glimcher, P.W., 2005. Midbrain dopamine neurons encode a quantitative reward prediction error signal. Neuron 47, 129–141.
Behrens, T.E., Woolrich, M.W., Walton, M.E., Rushworth, M.F., 2007. Learning the value of information in an uncertain world. Nat. Neurosci. 10, 1214–1221.
Bode, S., Haynes, J.D., 2009. Decoding sequential stages of task preparation in the human brain. NeuroImage 45, 606–613.
Breiter, H.C., Aharon, I., Kahneman, D., Dale, A., Shizgal, P., 2001. Functional imaging of neural responses to expectancy and experience of monetary gains and losses. Neuron 30, 619–639.
Chib, V.S., Rangel, A., Shimojo, S., O'Doherty, J.P., 2009. Evidence for a common representation of decision values for dissimilar goods in human ventromedial prefrontal cortex. J. Neurosci. 29, 12315–12320.
Cohen, M.X., 2008. Neurocomputational mechanisms of reinforcement-guided learning in humans: a review. Cogn. Affect. Behav. Neurosci. 8, 113–125.
Cohen, M.X., Elger, C.E., Weber, B., 2008. Amygdala tractography predicts functional connectivity and learning during feedback-guided decision-making. NeuroImage 39, 1396–1407.
Daw, N.D., O'Doherty, J.P., Dayan, P., Seymour, B., Dolan, R.J., 2006. Cortical substrates for exploratory decisions in humans. Nature 441, 876–879.
FitzGerald, T.H., Seymour, B., Dolan, R.J., 2009. The role of human orbitofrontal cortex in value comparison for incommensurable objects. J. Neurosci. 29, 8388–8395.
Glascher, J., Hampton, A.N., O'Doherty, J.P., 2009. Determining a role for ventromedial prefrontal cortex in encoding action-based value signals during reward-related decision making. Cereb. Cortex 19, 483–495.
Gold, J.I., Shadlen, M.N., 2007. The neural basis of decision making. Annu. Rev. Neurosci. 30, 535–574.
Goldman-Rakic, P., 1987. Circuitry of primate prefrontal cortex and regulation of behavior by representational memory. In: Mountcastle, V.B., Plum, F., Geiger, S.R. (Eds.), Handbook of physiology: the nervous system. American Physiology Society, Bethesda, MD, pp. 373–417.
Gottfried, J.A., O'Doherty, J., Dolan, R.J., 2003. Encoding predictive reward value in human amygdala and orbitofrontal cortex. Science 301, 1104–1107.
Hampton, A.N., O'Doherty, J.P., 2007. Decoding the neural substrates of reward-related decision making with functional MRI. Proc. Natl. Acad. Sci. U. S. A. 104, 1377–1382.
Hampton, A.N., Bossaerts, P., O'Doherty, J.P., 2006. The role of the ventromedial prefrontal cortex in abstract state-based inference during decision making in humans. J. Neurosci. 26, 8360–8367.
Hare, T.A., Camerer, C.F., Rangel, A., 2009. Self-control in decision-making involves modulation of the vmPFC valuation system. Science 324, 646–648.
Haynes, J.D., Rees, G., 2005. Predicting the orientation of invisible stimuli from activity in human primary visual cortex. Nat. Neurosci. 8, 686–691.
Haynes, J.D., Rees, G., 2006. Decoding mental states from brain activity in humans. Nat. Rev. Neurosci. 7, 523–534.
Haynes, J.D., Sakai, K., Rees, G., Gilbert, S., Frith, C., Passingham, R.E., 2007. Reading hidden intentions in the human brain. Curr. Biol. 17, 323–328.
Heekeren, H.R., Marrett, S., Bandettini, P.A., Ungerleider, L.G., 2004. A general mechanism for perceptual decision-making in the human brain. Nature 431, 859–862.
Heekeren, H.R., Marrett, S., Ungerleider, L.G., 2008. The neural systems that mediate human perceptual decision making. Nat. Rev. Neurosci. 9, 467–479.
Kable, J.W., Glimcher, P.W., 2007. The neural correlates of subjective value during intertemporal choice. Nat. Neurosci. 10, 1625–1633.
Kahnt, T., Park, S.Q., Cohen, M.X., Beck, A., Heinz, A., Wrase, J., 2009. Dorsal striatal–midbrain connectivity in humans predicts how reinforcements are used to guide decisions. J. Cogn. Neurosci. 21, 1332–1345.
Kahnt, T., Heinzle, J., Park, S.Q., Haynes, J.D., 2010. The neural code of reward anticipation in human orbitofrontal cortex. Proc. Natl. Acad. Sci. U. S. A. 107, 6010–6015.
Kamitani, Y., Tong, F., 2005. Decoding the visual and subjective contents of the human brain. Nat. Neurosci. 8, 679–685.
Kennerley, S.W., Dahmubed, A.F., Lara, A.H., Wallis, J.D., 2009. Neurons in the frontal lobe encode the value of multiple decision variables. J. Cogn. Neurosci. 21, 1162–1178.
Kim, H., Shimojo, S., O'Doherty, J.P., 2006. Is avoiding an aversive outcome rewarding? Neural substrates of avoidance learning in the human brain. Public Libr. Sci. Biol. 4, e233.
Knutson, B., Rick, S., Wimmer, G.E., Prelec, D., Loewenstein, G., 2007. Neural predictors of purchases. Neuron 53, 147–156.
Kobayashi, S., Pinto de, C.O., Schultz, W., 2010. Adaptation of reward sensitivity in orbitofrontal neurons. J. Neurosci. 30, 534–544.
Kriegeskorte, N., Goebel, R., Bandettini, P., 2006. Information-based functional brain mapping. Proc. Natl. Acad. Sci. U. S. A. 103, 3863–3868.
Lattal, K.M., Nakajima, S., 1998. Overexpectation in appetitive Pavlovian and instrumental conditioning. Anim. Learn. Behav. 26, 351–360.
McClure, S.M., Berns, G.S., Montague, P.R., 2003. Temporal prediction errors in a passive learning task activate human striatum. Neuron 38, 339–346.
Montague, P.R., Berns, G.S., 2002. Neural economics and the biological substrates of valuation. Neuron 36, 265–284.
Montague, P.R., Hyman, S.E., Cohen, J.D., 2004. Computational roles for dopamine in behavioural control. Nature 431, 760–767.
Morrison, S.E., Salzman, C.D., 2009. The convergence of information about rewarding and aversive stimuli in single neurons. J. Neurosci. 29, 11471–11483.
Norman, K.A., Polyn, S.M., Detre, G.J., Haxby, J.V., 2006. Beyond mind-reading: multi-voxel pattern analysis of fMRI data. Trends Cogn. Sci. 10, 424–430.
O'Doherty, J.P., Dayan, P., Friston, K., Critchley, H., Dolan, R.J., 2003a. Temporal difference models and reward-related learning in the human brain. Neuron 38, 329–337.
O'Doherty, J.P., Critchley, H., Deichmann, R., Dolan, R.J., 2003b. Dissociating valence of outcome from behavioral control in human orbital and ventral prefrontal cortices. J. Neurosci. 23, 7931–7939.
Ollinger, J.M., Shulman, G.L., Corbetta, M., 2001. Separating processes within a trial in event-related functional MRI. NeuroImage 13, 210–217.
Padoa-Schioppa, C., Assad, J.A., 2006. Neurons in the orbitofrontal cortex encode economic value. Nature 441, 223–226.
Pessiglione, M., Seymour, B., Flandin, G., Dolan, R.J., Frith, C.D., 2006. Dopamine-dependent prediction errors underpin reward-seeking behaviour in humans. Nature 442, 1042–1045.
Plassmann, H., O'Doherty, J., Rangel, A., 2007. Orbitofrontal cortex encodes willingness to pay in everyday economic transactions. J. Neurosci. 27, 9984–9988.
Rescorla, R.A., 1970. Reduction in effectiveness of reinforcement after prior excitatory conditioning. Learn. Motiv. 1, 372–381.
Romo, R., Salinas, E., 2003. Flutter discrimination: neural codes, perception, memory and decision making. Nat. Rev. Neurosci. 4, 203–218.
Romo, R., Brody, C.D., Hernandez, A., Lemus, L., 1999. Neuronal correlates of parametric working memory in the prefrontal cortex. Nature 399, 470–473.
Schoenbaum, G., Saddoris, M.P., Stalnaker, T.A., 2007. Reconciling the roles of orbitofrontal cortex in reversal learning and the encoding of outcome expectancies. Ann. NY Acad. Sci. 1121, 320–335.
Schultz, W., Dayan, P., Montague, P.R., 1997. A neural substrate of prediction and reward. Science 275, 1593–1599.
Slovic, P., Fischhoff, B., Lichtenstein, S., 1977. Behavioral decision-theory. Annu. Rev. Psychol. 28, 1–39.
Soon, C.S., Brass, M., Heinze, H.J., Haynes, J.D., 2008. Unconscious determinants of free decisions in the human brain. Nat. Neurosci. 11, 543–545.
Sutton, R., Barto, A., 1998. Reinforcement learning: an introduction. MIT Press, Cambridge, MA.
Takahashi, Y.K., Roesch, M.R., Stalnaker, T.A., Haney, R.Z., Calu, D.J., Taylor, A.R., Burke, K.A., Schoenbaum, G., 2009. The orbitofrontal cortex and ventral tegmental area are necessary for learning from unexpected outcomes. Neuron 62, 269–280.
von Winterfeldt, D., Fischer, G.W., 1975. Multi-attribute utility theory: models and assessment procedures. In: Wendt, D., Vlek, C.A.J. (Eds.), Utility, probability, and human decision making. Reidel, Dordrecht, The Netherlands, pp. 47–86.
Yacubian, J., Glascher, J., Schroeder, K., Sommer, T., Braus, D.F., Buchel, C., 2006. Dissociable systems for gain- and loss-related value predictions and errors of prediction in the human brain. J. Neurosci. 26, 9530–9537.
Zysset, S., Wendt, C.S., Volz, K.G., Neumann, J., Huber, O., von Cramon, D.Y., 2006. The neural implementation of multi-attribute decision making: a parametric fMRI study with human subjects. NeuroImage 31, 1380–1388.